CFD Modelling and Experimental Validation of a Single-Slope Passive Solar Still for Efficient Water Desalination

Mani Saraswathi Hallika Pindiprolu[1], *Vishwanath* Kumar Panangipalli[2*], *Chivukula* V S D Kartheek[2]

[1]Department of Mechanical Engineering, G. Narayanamma Institute of Technology and Science (for Women), Hyderabad, Telangana 500104, India
[2]Department of Mechanical Engineering, Anurag University, Hyderabad, Telangana 500088, India.

Abstract. Water, vital for life, is largely unusable despite being renewable. Growing populations, urbanization, and pollution continually deplete the world's drinking water supply. A third of the global population faces freshwater scarcity. Natural sources can't fully meet demand, necessitating efficient water desalination. Solar stills, utilizing solar desalination, offer a low-energy solution, particularly beneficial in electricity-deprived rural areas. However, their potable water output remains a challenge. Hence, research on modelling and transport factors is essential for enhancing solar still design efficiency". In this study, a multi-phase two-dimensional model of a single slope passive solar still was developed using Fluent, ANSYS 19.2. Using the simulated data, the solar still's performance was evaluated against experimental data. The simulation model predicted a maximum distillate output of 0.0692 kg/m^2.hr, which closely aligned with the experimental value of 0.58 kg/m^2.hr, indicating strong agreement between the simulation and experimental results. The error percentage in terms of water temperature between the simulated and experimental results was found to be 1.55%."

Keywords: Solar desalination, Solar still, Multiphase flow, Solar energy, ANSYS Fluent, CFD.

1 Introduction

Water is a very valuable gift of Mother Nature. Two-thirds portion of the earth's surface is covered with water. 97% of the water body is salty in the form of seas and glaciers while only 2.6% is freshwater (rivers, lakes, and reservoirs) of which less than 1% of fresh water is available to support life and vegetation [1]. However, the rapid rise in population and industrial development led to the depletion of freshwater resources [2]. This poses a significant challenge as over 780 million people worldwide are currently affected by water shortages [3]. As per the "22nd GWI/IDA Worldwide Desalting Plant Inventory", it was

* Corresponding author email – vishwanathmech@anurag.edu.in

reported that the global daily freshwater production is 60 million m^3 from 14,451 desalination plants [4]. Although desalination is an old way of converting brackish and saline water into freshwater, there is a lot of scope in the research due to the shortage of freshwater availability together with increasing demand for it.

1.1 Solar Still

A solar still, operating on the principle of solar distillation, serves as a device that generates potable water directly for human consumption. Solar stills emerge as highly effective alternatives to provide clean water in distant villages where there is limited access to electricity. Functioning as stationary devices, solar stills harness the thermal energy from sunlight for water purification. Solar energy, being abundant and green, positions solar stills as optimal among renewable energy sources. The typical operation of solar still involves utilizing solar energy to heat liquid water, causing it to evaporate and form vapor. This vapor then undergoes condensation on a tilted glass cover, resulting in the collection of condensed water as potable water. In recent years, researchers have done many experimental, numerical, and analytical studies on various still designs to improve the distillate output [5]. These designs are broadly divided into single-effect and multi-effect stills. Furthermore, they are termed as active or passive based on the heat source [5]. In passive mode, basin water gets heated by solar radiation, while in active mode, heating is done through additional sources namely solar collectors, concentrators, and heaters [6–8].

1.2 Application of Computational Fluid Dynamics (CFD) in Solar Stills.

In recent times, CFD numerical simulations have gained widespread application for studying the operational mechanisms of various solar still systems. This is due to its capability to generate results within complex systems where experimental work may be challenging to conduct at a substantially low time and cost [9]. Various simulation models have been developed by researchers and are validated with experiments. El-Sebaey et al. [10] have modeled a Volume of Fraction (VOF) model of a single slope solar still and have studied the temperature variations, fluid and vapor fraction, productivity, and mixture velocity contours. Their model has been validated with their experiments with an error of 8.3%. Rahbar et al. [11] have performed a theoretical and numerical analysis on a single slope solar still using ANSYS Fluent. The authors reported a maximum error of 12.5% between theory and simulation. Malaiyappan and Elumalai [12] conducted tests on a single-slope solar still and validated with simulations using ANSYS CFX. The authors reported that CFD could accurately predict the distillate yield with an average error of 5.26% for the same simulated experimental conditions. In addition, it was predicted that a solar still with aluminum as the basin material could produce highest yield as compared to galvanized iron and glass. Rahbar et al. [13] studied tests on triangular and tubular solar stills along with the CFD model. The estimated distillate yield using CFD is with a maximum error of 6.1% as compared to experimental observations [13]. The research on studying solar still efficiency using CFD is increasing every year. Looking at the trend, a lower number of publications is evident in the period between 2012 and 2019, with approximately 46.5% of the total works being published in the first 8 years. The maximum number of articles, five, was published in 2018, while the highest count, 12 articles, occurred in 2020. Notably, over 53% of the articles were published in the most recent 3 years (2020–2022). This indicates a notable increase in the utilization of CFD for analyzing solar still performance. This surge is due to developments in numerical approaches and substantial improvements in computer capacity [14].

To summarize, Computational Fluid Dynamics (CFD) is a valuable tool for assessing the efficiency of solar stills. Its capability to conduct essential analyses on the physical aspects of a computer system and numerical approaches makes it a useful asset. However, it's worth noting that studies utilizing CFD for solar still efficiency evaluation are currently limited [9]. As discussed earlier, the key advantage of using CFD in modeling Solar still systems allows for virtual testing and optimization, reducing the need for extensive physical prototypes and accelerating the design process. However, as per the numerical versus experimental analysis that has been performed in various works that have been discussed in this section, it is observed that the deviation of simulation results compared to the experimental results is high. Therefore, the primary objective of this paper is to minimize the error percentage between the experimental setup and computational simulations. While existing literature predominantly delves into CFD modeling using various multiphase flow models and designs, this study emphasizes the crucial impact of meshing on simulation performance. Furthermore, a notable aspect is that many models have focused solely on convective heat transfer, overlooking the significance of incorporating solar load models for more precise outcomes. To enhance the accuracy of CFD models, a comprehensive grid independence study has been executed to establish an optimal grid yielding superior results. Additionally, a solar load model has been incorporated to assess the radiation effects from the sun within the computational domain, aiming for results that closely align with real-life solar still systems.

2 Mathematical Modeling

2.1 Heat Transfer

The heat transfer inside the solar still is via convection, evaporation, and radiation. These modes influence the distillate productivity from the still and the still efficiency [15]. As the temperatures inside still lie between 25 to 600° C, Dunckle's model can be used for evaluating the convective heat transfer coefficient (h_{cw}) from basin water to the glass cover.

$$h_{cw} = 0.884\left[T_w - T_g + \frac{(P_w - P_g)(T_w + 273)}{268900 - P_w}\right]^{1/3} \quad (1)$$

where,

$$P_w = exp\left(25.317 - \frac{5144}{T_w + 273}\right) \quad (2)$$

$$P_g = exp\left(25.317 - \frac{5144}{T_g + 273}\right) \quad (3)$$

From the eq. (1), the heat transfer due to convection is written as:

$$q_{cw} = h_{cw}(T_w - T_g) \quad (4)$$

The heat transfer coefficient due to evaporation (h_{ew}) is taken from Seetodesh et al. [16]:

$$h_{ew} = 0.016273(h_{cw})\left(\frac{P_w - P_g}{T_w - T_g}\right) \quad for\ lower\ temperature\ ranges \quad (5)$$

$$h_{ew} = 0.008(h_{cw})\left(\frac{P_w - P_g}{T_w - T_g}\right) for\ higher\ temperature\ ranges \quad (6)$$

From the eq. (4) and eq. (5), the heat transfer due to evaporation is written as:

$$q_{ew} = h_{ew}(T_w - T_g) \quad (7)$$

The heat transfer coefficient due to radiation (h_{rw}) is taken from Seetodesh et al. [16]:

$$h_{rw} = \varepsilon_{eff}\sigma\left[(T_w + 273)^2 + (T_g + 273)^2\right]\left[T_w + T_g + 546\right] \quad (8)$$

where, $\varepsilon_{eff} = \frac{1}{\varepsilon_g} + \frac{1}{\varepsilon_w} - 1$

The hourly yield of a single-slope solar still can be expressed as:

$$\dot{m}_{hourly} = \frac{q_{ew}}{h_{fg}} \times 3600 \times A_{eff} \quad (9)$$

Although Dunkle's model is accurate enough to estimate the solar still's performance under low temperatures, it is limited to certain approximations listed in Subhashini and Nigam [17].

3 Simulation

3.1 Geometric Modelling and Meshing

The geometry of the two-dimensional solar still is created in Ansys Design modeler as shown in Fig. 1. The still has a base area of 1m x 1m with a glass cover at an inclination of 17°.

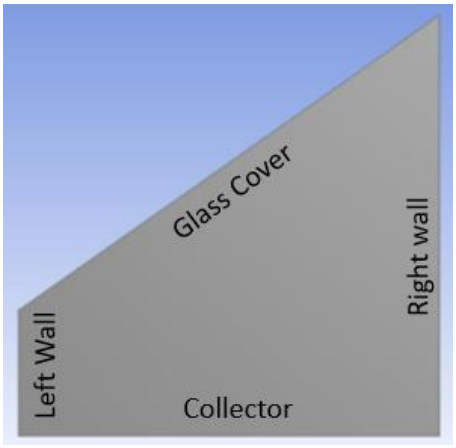

Fig. 1. 2D Geometric model of the solar still

The geometry creation is followed by mesh generation. Meshing is nothing but dividing the computational domain into multiple cells. The cell number depends on the necessity of the simulation accuracy and the associated computational time. An optimum mesh would ensure better accuracy within the limited time, but it is based on the complexity of the physical problem. Fig. 2 shows the generated mesh for the solar still computational domain.

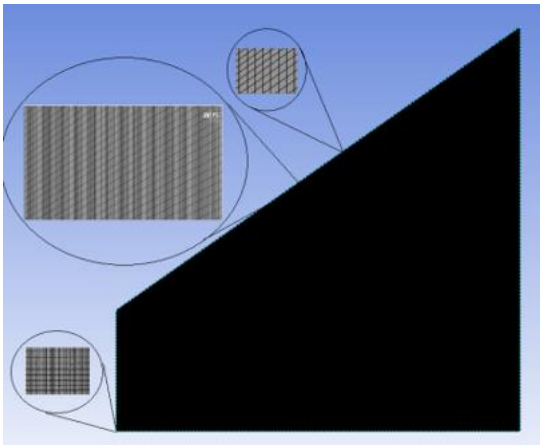

Fig. 2. Generated Mesh

Mesh Quality. A high-quality mesh is crucial for accurate CFD analysis. This study opted for a hexahedral mesh due to the solar still's predominantly rectangular surfaces, offering accuracy with moderate computation time. The mesh contained 100229 elements, sufficient for the problem's complexity. After mesh generation, assessing mesh quality is vital, as it directly impacts solution accuracy. Parameters like skewness and aspect ratio were evaluated; skewness values close to zero indicate good quality elements, with an average skewness below 0.3 desired. The skewness graph shown in Fig. 3 reveals that the computational domain has good-quality mesh with the majority of the mesh elements having skewness less than 0.3. Aspect ratio is another crucial parameter for evaluating mesh quality. A desirable average aspect ratio for a high-quality mesh is below 2. The aspect ratio graph represented in Fig. 4 indicates that the majority of elements have an aspect ratio below 2. These mesh results confirm that a predominantly hexahedral mesh is of good quality. Finally, a grid-independence study is essential to generate an optimum mesh. This is done by iterating the simulations for varied mesh sizes to achieve stability in the selected output parameter. This is discussed in Section 5.1.

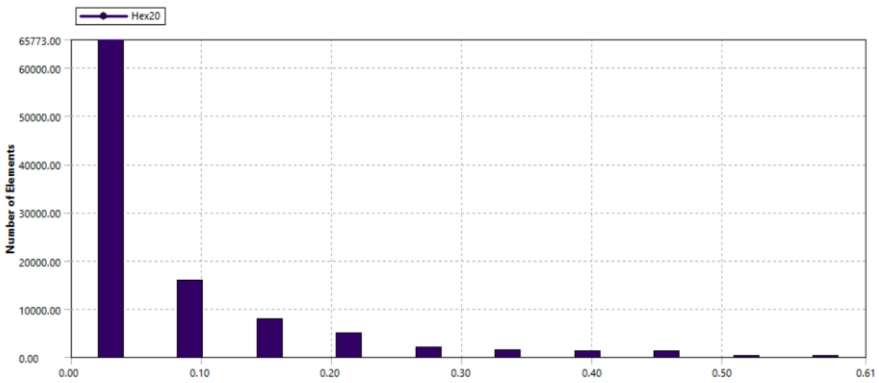

Fig. 3. Skewness of the mesh elements

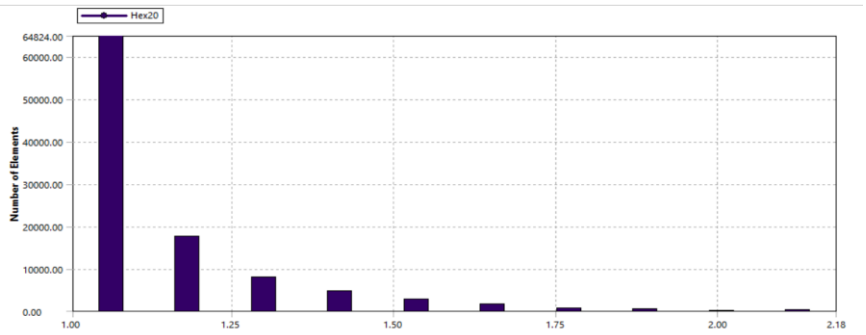

Fig. 4. Aspect ratio of the mesh elements

3.2 Governing Equations

Following the simulation method adopted by El-Sebaey et al. [10], all the governing equations used for the mixture phase are listed below.

3.2.1 Energy Equation

$$\frac{\partial}{\partial t}\sum_{k=1}^{n}\left(\alpha_k\rho_k E_k + \nabla\cdot\sum_{k=1}^{n}\left(\alpha_k \underline{v}_k(\rho_k E_k + P)\right)\right) = \nabla\cdot\left(K_{eff}\nabla T\right) + S_E \qquad (10)$$

where K_{eff} is the effective conductivity.

3.2.2 Continuity Equation

$$\frac{\partial}{\partial t}(\rho_m) + \nabla\cdot(\rho_m\overline{v_m}) = 0 \qquad (11)$$

where, $\overline{v_m}$ is the mass-averaged velocity:

$$\overline{v_m} = \frac{\sum_{k=1}^{n}\alpha_k\rho_k\overline{v_k}}{\rho_m} \qquad (12)$$

3.2.3 Momentum Equation

$$\frac{\partial}{\partial t}(\rho_m\overline{v_m}) + \nabla\cdot(\rho_m\overline{v_m}\,\overline{v_m}) = -\nabla p + \nabla\cdot\left[\mu_m\left(\nabla\overline{v_m} + \nabla\overline{v_m}^{T}\right)\right] + \rho_m\bar{g} + \bar{F} + \nabla\cdot\left(\sum_{k-1}^{n}\alpha_k\rho_k\bar{v}_{dr,k}\bar{v}_{dr,k}\right) \qquad (13)$$

To predict the intensity of incident radiation and atmospheric temperature for specified latitude and altitude conditions, the Rosseland model is selected in combination with solar ray tracing and solar loading.

3.3 CFD Analysis

Passive single-slope solar still is analyzed considering these assumptions: insulated side walls, negligible inlet air velocity, constant liquid and solid properties, film-wise condensation, no wind velocity effects, and no variation of temperature within the glass cover and the basin water. Table 1 summarizes the boundary conditions. Table 2 presents the

physical and thermal properties of the fluid (air) and the materials. Table 3 indicates other simulation parameters.

Table 1. Simulation Conditions at various boundary zones of the computational domain

Name of the Zone	Boundary Type	Simulation Conditions
Collector (copper)(opaque)	wall	Constant temperature, radiation
Glass (semi-transparent)	wall	Constant temperature, Radiation
Wall boundaries (opaque)	wall	Adiabatic

Table 2. Physical and thermal properties of the materials

Material	Density (kg/m^3)	Specific heat capacity (J/kg K)	Thermal conductivity (W/m K)
Air	1.225	1006	0.0242
Glass	2235	750	1.15
Copper	7196	502	55

Table 3. Input parameters used in the simulation

Input Parameter	Description
Solver	2D domain, transient and implicit 1st order k-ε model, standard wall function Mixture Model Roseeland radiation model, Solar loading
Materials	Solid: Copper, Glass Fluid: Air, water-vapor, water-liquid,
Phases	Primary: Air Secondary: Water-vapor, Water-liquid
Operating pressure	1.01 bar
Gravity	Y - Direction
Operation temperature	288.16 K

4 Experimentation

A single slope passive solar still is fabricated with the effective area scaled down to 0.0635m^2. Fig. 5 (a) and Fig. 5 (b) indicate the fabrication process of the solar still. The walls of the still are made of wood to minimize heat losses. The glass cover thickness is 5mm. The bottom basin (absorber plate) is made of a 1 mm thick aluminum sheet. Thermocouples were installed on the glass surface, absorber plate, and inside the water, as seen in Fig. 6 (a), and a multimeter as seen in Fig. 6 (b) to measure the temperatures. A collector trough is made using a PVC pipe and installed with a slope for the water to drain into the outlet. The trough can be seen in Fig. 5(a). A beaker is used to collect the distilled water and to measure the distillate output. Thermocouples are placed at the glass cover, absorber plate, and the water surface to record the respective temperatures.

(a) (b)

Fig. 5. Making of the Solar Still: (a) Enamel Coating of the absorber surface, (b) Collection trough

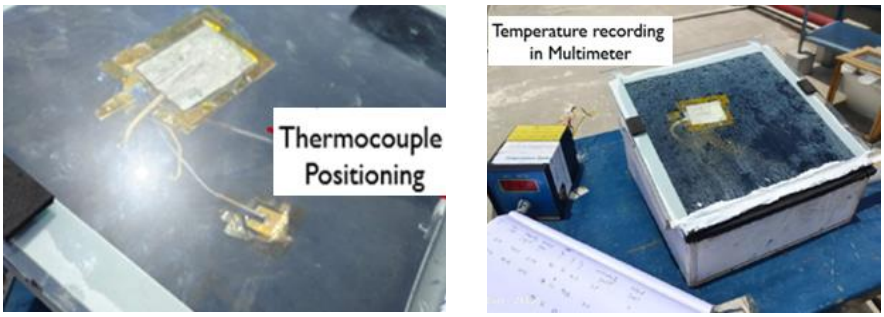

(a) (b)

Fig. 6. Temperature measurement: (a) Thermocouples arrangement, (b) Temperature recording using multimeter

5 Results and Discussion

5.1 Grid Independence Study

To select the appropriate mesh size, this study has been performed. In general, the finer the mesh, the more accurately one can capture the contours of a geometry. Fig. 7 shows the results of the grid independence study. Initially, for the mesh containing 143,856 elements the maximum y direction velocity of water from the absorber plate is very aggressive. But the value suddenly declines as the mesh element size is decreased. After 3 iterations, it can be observed that the velocity value has been stable. Therefore, the mesh containing 242003 elements has been chosen to perform the simulation.

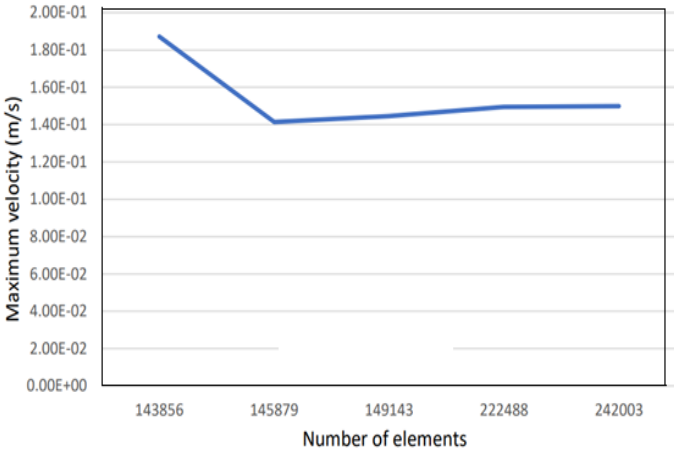

Fig. 7. Grid Independence Study

5.2 CFD Simulation Results

The accurate prediction of distillate yield from the solar still is dependent on the difference in temperature between the basin liner and the glass cover. Hence, it is critical to estimate the temperatures of the still interior, basin water, and glass cover through CFD simulation. The contours of temperatures within the still are depicted on the X-Y plane from the still center along the walls. Temperature values between 314 K and 360 K were selected to represent contours. The simulation ran from 8:00 AM to 5:00 PM (17:00). Fig. 8 and Fig. 9 represent the temperature contours between 9:00 AM and 2:00 PM (14:00). The temperature contours of the solar still interior illustrate the following: Initially, as solar radiation reaches the basin, water temperature begins to increase. Over time, the water heats up, leading to evaporation and subsequent vapor formation within the still, consequently raising the interior temperature. These contours demonstrate a progressive increase in the interior temperature with time, correlating directly with the intensity of solar radiation. The interior temperature peaks around 1:00 PM (13:00) and declines gradually. The temperature trend inside the still resembles the variation of solar radiation incident on the glass cover. Notably, the temperature distribution within the still appears uniform due to the occupying space of hot vapors after an hour of operation.

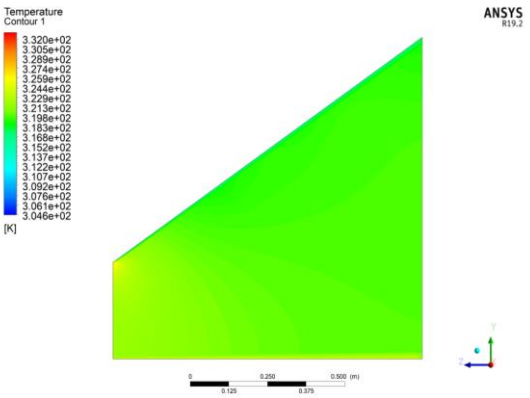

Fig. 8. Temperature contours at 9:00 AM

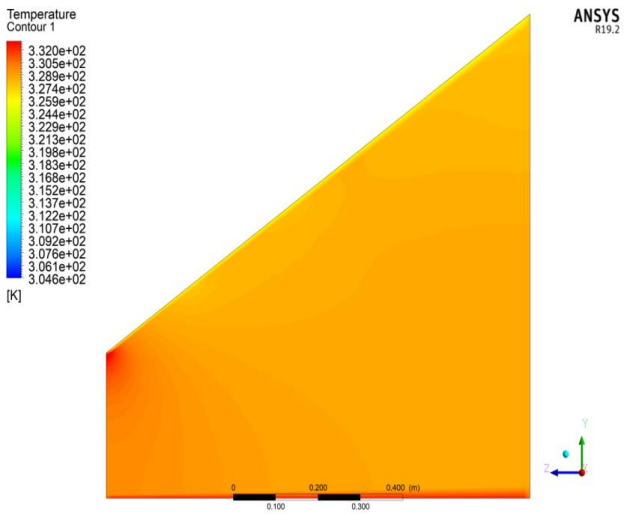

Fig. 9. Temperature contours at 2:00 PM (14:00)

Additionally, water volume fraction contours depict the initiation of evaporation by 9:00 AM, as evidenced in Fig. 10, with further vaporization observed between 1:00 PM (13:00) and 2:00 PM (14:00), as depicted in Fig. 11, coinciding with maximum absorber plate temperature, indicating water particles transitioning into vapor and evaporating towards the glass cover.

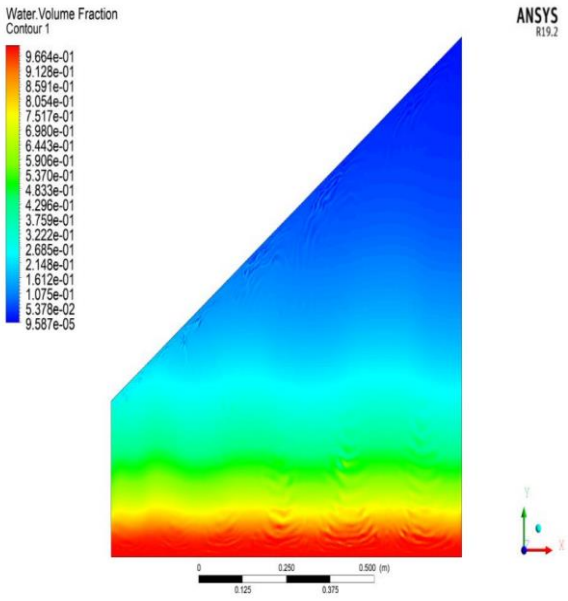

Fig. 10. Water volume fraction contour at 9:00 AM

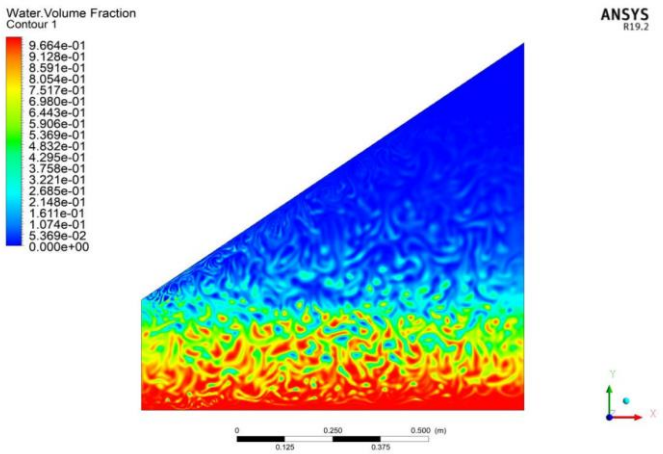

Fig. 11. Water volume fraction contour at 2:00 PM (14:00)

5.3 Experimental Data Validation

In Fig. 12, the predicted water temperatures from the ANSYS Fluent simulation are compared with experimental data. The graph illustrates that the water temperature increases until 1:00 PM (13:00), attributed to the ample availability of solar insolation providing heat energy. However, after 1 pm, the temperature gradually decreases. The average error percentage of the simulated water temperature is calculated to be 1.55% as compared to experimental data. This variation is considered reasonable reinforcing the reliability of the computational model in accurately representing the physical behavior of the system.

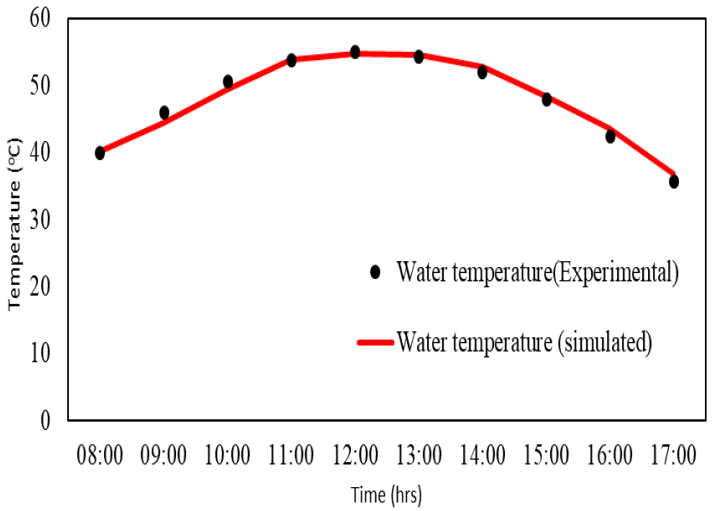

Fig. 12. Hourly Variation of Experimental and Simulated Basin Water Temperature

In the same way, the comparison plots of temperatures of the absorber plate and glass cover are shown in Fig. 13 and Fig.14. In a solar still, condensation occurs on the inner glass cover. Experimental observations indicate that distillate yield increases with increasing temperature difference between the water and the glass cover. This relationship underscores the importance of maintaining a significant temperature gradient between the water surface and the inner glass cover. This could lead to an increased rate of condensation and the optimum distillate output.

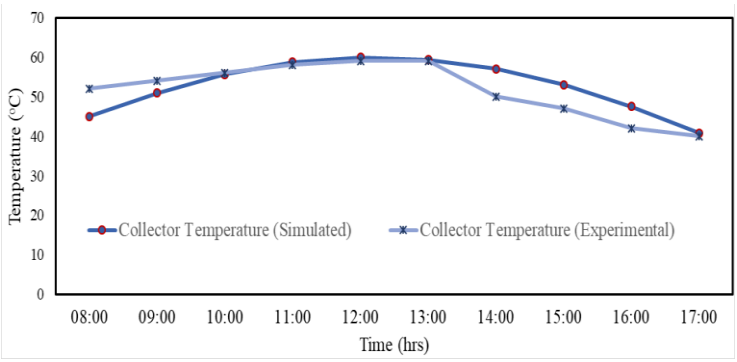

Fig. 13. Hourly Variation of Experimental and Simulated Collector (absorber plate) Temperature

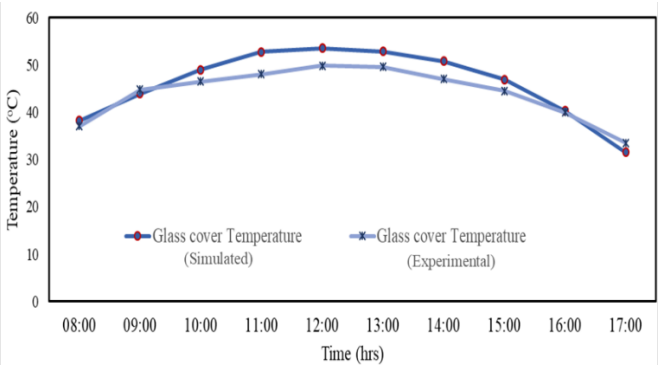

Fig. 14. Hourly Variation of Experimental and Simulated Glass Cover Inner Temperature

Certainly, heat transfer is a critical phenomenon required for distillate production in a solar still. In a solar still, the gas phase undergoes motion driven by buoyancy forces, leading to a natural convection process. This natural convection process is a consequence of temperature differences within the mixture. A MATLAB script is written to determine the distillate yield from the solar still based on the recorded temperature values. Fig. 15 visually depicts the variation in distillate output, showcasing a comparison between experimental and simulation results obtained using ANSYS Fluent. The distillate output predicted by the CFD model has a peak value of 0.6092 kg/m^2.hr at 2:00 PM (14:00) which closely matches the experimental observation of 0.58 kg/m^2.hr at the same time. The output trend gradually increases and reaches a maximum value at around 2:00 PM (14:00) and reaches its minimum value during the end of the simulation.

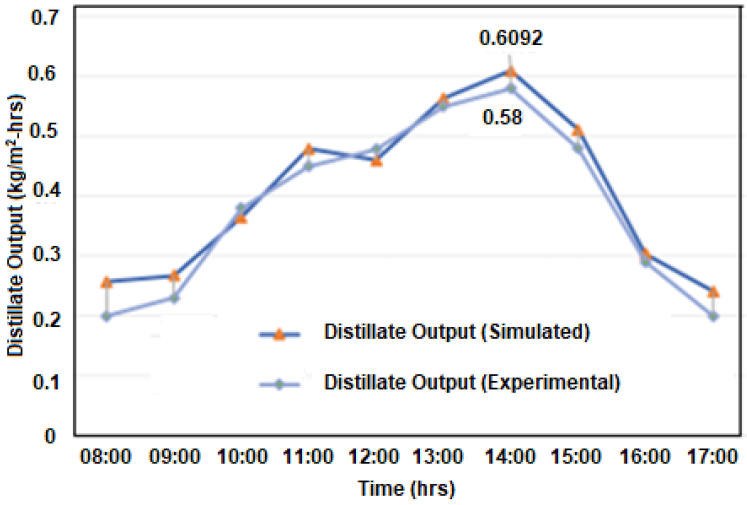

Fig. 15. Variation of Experimental and Simulated Distillate output with time

6 Conclusion

In this study, the process of evaporation and condensation in a solar still has been effectively simulated using ANSYS Fluent. The simulation involves a two-dimensional model that extends over a continuous period of 8 hours, divided into 8 steps of 1-hour duration each. An optimum and good quality mesh combined with Roseland radiation model ensured identical experimental conditions (incident solar radiation intensity, ambient temperature, location latitude and altitude) applied to the computational domain. The results obtained from the simulations exhibit good agreement with the corresponding experimental values of distilled water rate, glass cover temperature and basin water temperature. The maximum distillate output from experiments and simulation in the afternoon at 2 PM were found to be 0.58 and 0.6092 kg/m^2.hr respectively. The success in achieving the error percentage of 1.55% in terms of Water temperature of simulated and experimental results highlights the capability and accuracy of the CFD model in ANSYS Fluent in capturing the complex thermal and fluid dynamics within the solar still. The software emerges as a powerful tool not only for simulation but also for design, parameter analysis, and troubleshooting in the construction of solar stills.

References

1. Shankar P. and Kumar S., "Solar Distillation–A Parametric Review." VSRD International Journal of Mechanical, Automobile and Production Engineering, 2012, Vol. 2, pp : 17-33.
2. Kannan R., Selvaganesan C., Vignesh M., Babu B. R., Fuentes M., Vivar M., Skryabin I.,Srithar K. "Solar still with vapor adsorption basin: Performance analysis." Renewable Energy, 2014 ,Vol. 62 , pp: 258-264.
3. Bhardwaj R., Ten Kortenaar M. V. and Mudde R. F., "Influence of condensation surface on solar distillation." Desalination, 2016 ,326, pp: 37-45.
4. Xiao G., Xihui W., Mingjiang Ni, Fei W., Weijun Z., Zhongyang L., Kefa C. "A review on solar stills for brine desalination." Applied Energy,2012, 103, pp: 642-652.

5. Kumar, P.V.; Kumar, A.; Prakash, O.; Kaviti, A.K. Solar stills system design: A review. Renew. Sustain. Energy Rev. 2015, 51, pp:153–181.
6. Manokar, A.M.; Winston, D.P.; Kabeel, A.; El-Agouz, S.; Sathyamurthy, R.; Arunkumar, T.; Madhu, B.; Ahsan, A. Integrated PV/T solar still- A mini-review. Desalination 2018, 435, pp:259–267.
7. Abimbola, T.O.; Takaijudin, H.; Singh, B.S.M.; Yusof, K.W.; Abdurrasheed, A.S.; Al-Qadami, E.H.H.; Isah, A.S.; Wong, K.X.; Nadzri, N.F.A.; Ishola, S.A.; et al. Comprehensive passive-mode performance analysis on a new multiple-mode solar still for sustainable clean water processing. J. Clean. Prod. 2021, 334, 130214.
8. Sharshir, S.; Kandeal, A.; Ismail, M.; Abdelaziz, G.; Kabeel, A.; Yang, N. Augmentation of a pyramid solar still performance using evacuated tubes and nanofluid: Experimental approach. Appl. Therm. Eng. 2019, 160, 113997.
9. Kabeel, A.; El-Said, E.M.; Abdulaziz, M. Computational fluid dynamic as a tool for solar still performance analysis and design development: A review. Desalination Water Treat. 2019, 159,pp: 200–213
10. El-Sebaey, M.S.; Ellman, A.; Hegazy, A.; Ghonim, T. Experimental analysis and CFD modeling for conventional basin-type solar still. Energies 2020, 13, 5734.
11. Rahbar, N.; Esfahani, J.A. Estimation of convective heat transfer coefficient in a single-slope solar still: A numerical study. Desalination Water Treat. 2012, 50, 387–396.
12. Malaiyappan, P.; Elumalai, N. Numerical investigations: Basin materials of a single-basin and single-slope solar still. Desalination Water Treat. 2015, 57, 21211–21233.
13. Rahbar, N.; Asadi, A.; Fotouhi-Bafghi, E. Performance evaluation of two solar stills of different geometries: Tubular versus triangular: Experimental study, numerical simulation, and second law analysis. Desalination 2018, 443, pp: 44–55.
14. AlSaleem, Saleem & Al-Qadami, Ebrahim & Zein, H. & Shafiquzzaman, Md & Haider, Husnain & Ahsan, Amimul & Alresheedi, Mohammad & Alghafis, Abdullah & Alharbi, Abdulaziz. (2022). Computational Fluid Dynamic Applications for Solar Stills Efficiency Assessment: A Review. Sustainability. 14. 10700. 10.3390/su141710700.
15. Panchal, Hitesh N, and Shah, P K. Modelling and verification of single slope solar still using ANSYS-CFX. Iraq: N. p., 2011. Web.
16. Setoodeh N., Rahimi R. and Ameri A. "Modeling and determination of heat transfer coefficient in a basin solar still using CFD." Desalination, 268, 2011, pp: 103-110.
17. Subhashini G. and Nigam K.D.P. ―CFD modeling of flow profiles and interfacial phenomena in two-phase flow in pipe, Chemical Engineering and Processing ,45, 2006, pp: 55–65.
18. Rosseland Radiation Model Theory.